Journal Pre-proof

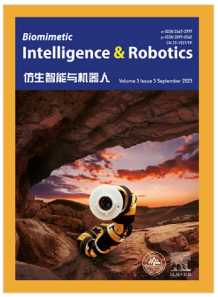

Computer-controlled ultra high voltage amplifier for dielectric elastomer actuators

Ardi Wiranata, Zebing Mao, Yu Kuwajima, Yuya Yamaguchi, Muhammad Akhsin Muflikhun, Hiroki Shigemune, Naoki Hosoya, Shingo Maeda

PII: S2667-3797(23)00053-0
DOI: https://doi.org/10.1016/j.birob.2023.100139
Reference: BIROB 100139

To appear in: *Biomimetic Intelligence and Robotics*

Received date : 28 September 2023
Revised date : 3 November 2023
Accepted date : 9 November 2023

Please cite this article as: A. Wiranata, Z. Mao, Y. Kuwajima et al., Computer-controlled ultra high voltage amplifier for dielectric elastomer actuators, *Biomimetic Intelligence and Robotics* (2023), doi: https://doi.org/10.1016/j.birob.2023.100139.

Computer-controlled Ultra High Voltage Amplifier for Dielectric Elastomer Actuators

Ardi Wiranata[a,*], Zebing Mao[b,*,1], Yu Kuwajima[c], Yuya Yamaguchi[c], Muhammad Akhsin Muflikhun[a], Hiroki Shigemune[d], Naoki Hosoya[e], Shingo Maeda[b,f]

[a] Department of Mechanical and Industrial Engineering, University of Gadjah Mada, Yogyakarta 55281, Indonesia.

[b] Department of Mechanical Engineering, Tokyo Institute of Technology, Tokyo 152-8550, Japan

[c] Department of Engineering and Science, Shibaura Institute of Technology, Tokyo 135-8548, Japan

[d] Department of Electrical Engineering, Shibaura Institute of Technology, Tokyo 135-8548, Japan

[e] Department of Engineering Science and Mechanics, Shibaura Institute of Technology, Tokyo 135-8548, Japan

[f] Living Systems Materialogy (LiSM) Research Group, International Research Frontiers Initiative (IRFI), Tokyo Institute of Technology, Yokohama 226-8501, Japan

***Corresponding author:** ardi.wiranata@ugm.ac.id, mao.z.aa@m.titech.ac.jp

[1] Given his role as Executive Guest Editor of this journal, Zebing Mao had no involvement in the peer-review of this article and had no access to information regarding its peer-review. Full responsibility for the editorial process for this article was delegated to Dr. Muhao Chen.

Abstract

Soft robotics is a breakthrough technology to support human-robot interactions. The soft structure of a soft robot can increase safety during human and robot interactions. One of the promising soft actuators for soft robotics is dielectric elastomer actuators (DEAs). DEAs can operate silently and have an excellent energy density. The simple structure of DEAs leads to the easy fabrication of soft actuators. The simplicity combined with silent operation and high energy density make DEAs interesting for soft robotics researchers. DEAs actuation follows the Maxwell-pressure principle. The pressure produced in the DEAs actuation depends much on the voltage applied. Common DEAs requires high voltage to gain an actuation. Since the power consumption of DEAs is in the milli-Watt range, the current needed to operate the DEAs can be neglected. Several commercially available DC-DC converters can convert the volt range to the kV range. In order to get a voltage in the 2-3kV range, the reliable DC-DC converter can be pricy for each device. This problem hinders the education of soft actuators, especially for a newcomer laboratory that works in soft electric actuators. This paper introduces an entirely do-it-yourself (DIY) Ultrahigh voltage amplifier (UHV-Amp) for education in soft robotics. UHV-Amp can amplify 12V to at a maximum of 4kV DC. As a demonstration, we used this UHV-Amp to test a single layer of powdered-based DEAs. The strategy to build this educational type UHV-Amp was utilizing a Cockcroft-Walton circuit structure to amplify the voltage range to the kV range. In its current state, the UHV-Amp has the potential to achieve approximately 4kV. We created a simple platform to control the UHV-Amp from a personal computer. In near future, we expect this easy control of the UHV-Amp can contribute to the education of soft electric actuators.

Keywords: Dielectric elastomer actuators, electric amplifier, soft actuators, soft robotics, soft actuator education

1. Introduction

Soft robotics is a new technology that accommodate human and robot interactions. Recently, some soft actuators in soft robotics have gained much attention from researchers and educators[1]. These soft actuators include soft pneumatic/hydraulic actuators[2][3], flexible pumps[4][5], soft electro-adhesion[6], a shape memory polymers[7], gel actuators[8][9], paper type soft robots[10] and dielectric elastomer actuators (DEAs)[11][12][13]. Each soft actuator has distinctive characteristics. For example, soft pneumatic actuators can produce a high actuation strain using a high-pressure air compressor. This high actuation strain can expand the application of soft actuators in some areas, such as the medical field[14] and the food industry[14][15]. This pneumatic soft-actuator can be fascinating for a researcher since the actuator can produce high actuation and high power output. Sample of the application of pneumatic actuators in the funabot-suit[16]. Funabot-suit apply the McKibben muscle principle to actuate the suit. Then, the other actuators, such as gel actuators and stretchable pumps, are also interesting technologies. However, these soft actuators also has some challenge including the pneumatic actuators require special equipment including air hoses and compressors [2] that potentially cause a complex setup in laboratory and require additional space. Then, for the gel actuator and stretchable pump, additional materials, such as special chemical and dielectric liquid, are required during the study. Some types of dielectric liquid for stretchable pumps and chemicals for gel actuators require special care since those materials can evaporate easily. This special treatment require special equipment that result in the additional cost during the experiment.

On the other hand, DEAs has a simple structure. DEAs consist of an elastomer membrane sandwiched between two stretchable electrodes (**Figure 1a** shows the structure of DEAs)[17][18]. DEAs works by connecting two stretchable electrodes to a DC power source. When the DC voltage is applied to the DEAs, the opposite charges accumulated at both of the DEAs electrodes. The opposite charge may trigger a Maxwell pressure (**Equations 1**) that squeeze the elastomer membrane in the thickness direction **(Figure 1b**). Since the elastomer membrane is incompressible, the DEAs expand in

the plane direction[19]. **Figure 1c** shows the basic single-layer DEAs. The amount of pressure generated by the two opposite charge at the DEAs electrodes follows the Maxwell pressure (*P*) equation (**Equation 1**) [19]. **Equation 1** describes the physics of the DEAs in a simple theoretical form. Based on the equation, changing some variables, such as the dielectric permittivity of material (ε), the thickness of the dielectric elastomer (*z*), characteristics of the material (*Y*), and voltage operation can change the actuation of DEAs (S_z). The simplicity of the DEAs structure can ease the researcher to prepare and develop new ideas on how to improve the actuation of DEAs. In educational side, educator or a trainer can easily prepare DEAs for teaching or training purpose. In the case of learning process in the laboratory, students can also have a hands-on project of DEAs, since the fabrication process is easy, fast, and simple. The combination of student involvement and a theoretical framework can boost the student understanding on the basics of soft actuators, especially electric-type actuators (e.g DEAs). This situation can accelerate the advances in dielectric elastomer technology.

$$P = \varepsilon_0 \varepsilon \left(\frac{V}{z}\right)^2 \quad (1)$$

$$S_z = \varepsilon_0 \varepsilon \frac{V^2}{Yz^2} \quad (2)$$

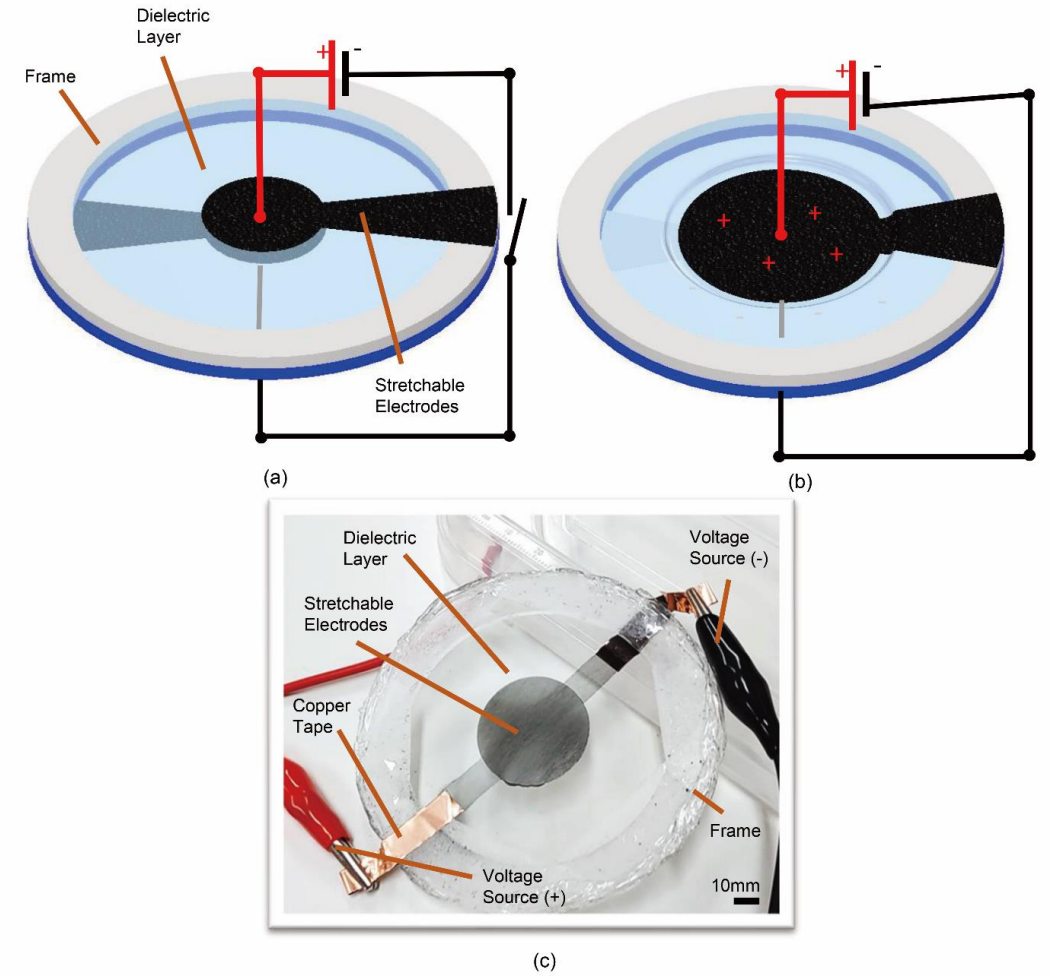

Figure 1. Dielectric Elastomer Actuator working principle and structure. (a. initial state, b. active state, c. dielectric elastomer actuator)

One major problem in the DEAs is that the device requires a high voltage for the actuation. There is a possibility to run DEAs in an ultralow voltage by reducing the elastomeric membrane to a nanometric thickness[12]. Reducing the thickness to nanometric thickness is a tough challenge. One possible solution to generate high voltage is using a professional high-voltage amplifier. Currently, a professional high-voltage amplifier is bulky and relatively high price[20]. There are commercially available DC-DC converters with small sizes[21][22]. This commercial DC-DC converter can be pricy and cause funding problems when multiple devices are required. In this case, a self-developed voltage amplifier can be helpful for newcomer researchers and laboratory activity. Generally, a voltage boosting technique can be divided into five main groups, including multistage[23], switched capacitor[24], voltage multiplier[25], magnetic coupling[26], and switched inductor and voltage lift[27]. Each voltage-boosting method has advantages and disadvantages. It depends on their application and functionality. For a hands-on project in the laboratory or class, a high-voltage amplifier should be compact, portable, low-cost, and user-friendly. The standard type of voltage multiplier, such as Cockcroft-Walton (CW), offers some benefits, including cost-effectiveness, the low voltage stress on capacitors and diodes, and a high voltage ratio. A completely Do-it-Yourself (DIY) device can be suitable for the learning process, students' hands-on projects, and a new soft robotics laboratory. DIY device has many advantages, including portability, cost effectiveness and can be customized to meet user requirements. Recently

DIY equipment is getting popular among researchers. DIY is an innovative activity of a researcher to create or produce equipment or process for a specific purpose[28]. Many laboratory equipment are a product of DIY, for example, a DIY calorimeter in a chemical laboratory[29][30], DIY data acquisition for chemical instrumentation[30], DIY microfluidics[31], a DIY chemical measurement device in a laboratory [32], DIY mannequin for blood collections [33], and DIY system for dynamic stem cell [34]. CW circuit is a potential circuit for DIY lab equipment since CW circuit has a relatively simple structure [35].

In this research, we focus on creating a shared toolkit and universal testing platform for a hands-on project of DEAs. The strategy is to use simple equipment that is commercially available in a marketplace. The main component of the UHV-Amp consists of Arduino micro as a main controller, L298N as a voltage controller, DC-AC inverter to create an AC voltage from a DC source, optocoupler as a rapid switch for high-frequency applications, capacitor, and diode. We used a Cockcroft Walton (CW) circuit to amplify the AC electricity to DC high voltage. John Cockcroft and Ernest Walton were the first developers of the CW circuit at the University of Cambridge in the early 1930s [36]. The original purpose of the CW circuit was for artificial atom splitting. In principle, a CW circuit consists of a ladder-structured network of capacitors and diodes. This circuit is useful to convert a regular voltage supplied by a household outlet to a high voltage (HV) through rectifying and filtering the alternating voltage[36]. We chose the CW circuit to build UHV-Amp because the CW circuit is a low-cost component, light in weight, and high portability. In order to ease the user to operate the UHV-Amp, we create a simple graphic user interface (GUI) using python. Since all of the equipment and GUI is an opensource and DIY friendly, we expect our platform to contribute much to soft robotics education in a classroom and laboratory. The general and universal toolkit for soft robotics can ease researcher to build upon equipment to support their research [37]. UHV-Amp also opens a new possibility of distance learning and distance laboratory, which can ease students to do their hands-on projects.

2. Materials and Methods

2.1. Cockcroft Walton (CW) circuit

A CW is a voltage multiplier circuit to convert a low voltage AC power source to dc High-Voltage (HV). CW requires a network of capacitors and diodes to amplify the voltage. CW has many advantages, such as the voltage in each stage is equal to twice of the peak input voltage (in a half-wave rectifier) and three times in a full-wave rectifier. In this case, the CW voltage only requires a relatively low-cost component[36]. We can also take the output voltage in every stage of the CW circuit [36]. Based on these advantages, the CW voltage can easily support the DEAs education either in class or in distance learning.

The design of the CW circuit should depend on the designer output voltage requirement. **Figure 2a** shows a basic CW circuit connected to an AC voltage input ($\pm V_i$). The detailed working principle of the CW circuit was reported by Brugler, et al [38]. In principle, *n-1* multiplying capacitors are needed to multiply the V_i by *n*. By assuming that the diodes are ideal, Brugler, et al [38] analyzed the CW circuit by considering the charge transfer at a steady state condition. When ΔQ is delivered to the load at n_{th} positive half cycle of voltage V_i , the charge was deposited on capacitor (C_1)during n – 1th negative half cycle, deposited on C_2 during n – 1th positive half cycle, and deposited on C_3 during n – 1th negative half cycle. These phenomena cause a coupled charge of ΔQ flow through the downward-directed diode in the positive phase and upward-directed diodes during the negative phase [38]. **Figure 2b** depicts the condition of V_i at a positive phase. **Figure 2b** also shows only the forward-biased diodes. **Figure 2c** describes the situation where V_i is in a negative state and only forward-biased diodes were presented in **Figure 2c.**

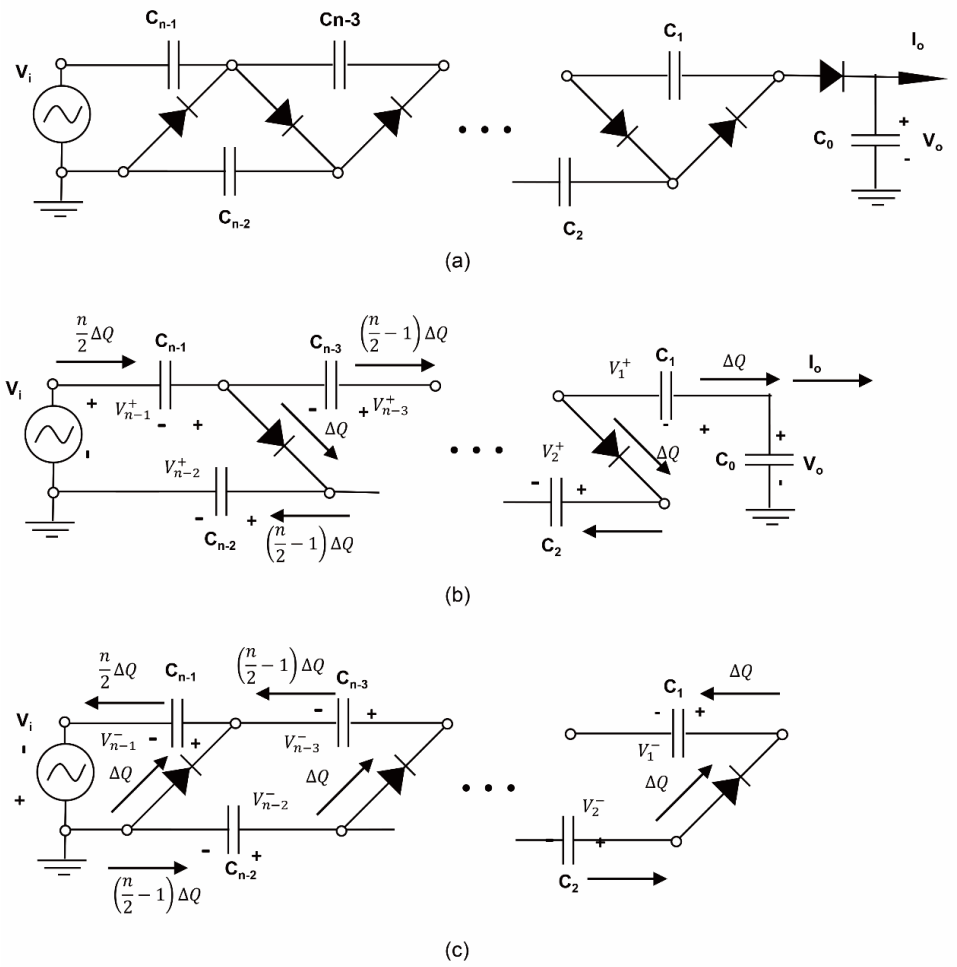

Figure 2. Basic CW circuit for voltage multiplier (a. basic CW circuit model, b. equivalent model at positive state of CW circuit, c. equivalent model at negative state of CW circuit)

The relationship between the output voltage and current is derived from **Figures 2b and 2c**. From **Figure 2c,** when V_i is in the negative half phase, the voltage $V_{n-1}^{-}$is described in **Equation 3.**

$$V_{n-1}^{-} = V_i \tag{3}$$

Charge $\frac{n}{2}\Delta Q$ is from C_{n-1}during the positive input transition then **Equation 4** should be

$$V_{n-1}^{+} = V_{n-1}^{-} - \frac{\frac{n}{2}\Delta Q}{C_{n-1}} = V_i \quad - \frac{\frac{n}{2}\Delta Q}{C_{n-1}} \tag{4}$$

Then V_{n-2}^{+} from **Figure 2b** is as follows (**Equation 5**):

$$V_{n-2}^{+} = V_i + V_{n-1}^{+} = 2V_i - \frac{\frac{n}{2}\Delta Q}{C_{n-1}} \tag{5}$$

After another half cycle

$$V_{n-2}^{-} = V_{n-2}^{+} \quad - \frac{\left(\frac{n}{2}-1\right)\Delta Q}{C_{n-2}} \tag{6}$$

$$V_{n-2}^{-} = 2V_i - \frac{\frac{n}{2}\Delta Q}{C_{n-1}} - \frac{\left(\frac{n}{2}-1\right)\Delta Q}{C_{n-2}} = V_{n-3}^{-} \quad (7)$$

By continuing the process, we can get :

$$V_{n-3}^{+} = V_{n-3}^{-} - \frac{\left(\frac{n}{2}-1\right)\Delta Q}{C_{n-3}} \quad (8)$$

$$V_{n-3}^{+} = 2V_i - \frac{\frac{n}{2}\Delta Q}{C_{n-1}} - \frac{\left(\frac{n}{2}-1\right)\Delta Q}{C_{n-2}} - \frac{\left(\frac{n}{2}-1\right)\Delta Q}{C_{n-3}} \quad (9)$$

By continuing the calculation process above, V^+ should be:

$$V^{+} = 2V_i - \frac{\frac{n}{2}\Delta Q}{C_{n-1}} - \frac{\left(\frac{n}{2}-1\right)\Delta Q}{C_{n-2}} - \frac{\left(\frac{n}{2}-1\right)\Delta Q}{C_{n-3}} \cdots - \frac{\Delta Q}{C_2} - \frac{\Delta Q}{C_2} \quad (10)$$

From **Figure 2b**, the total output voltage is the sum of V_i , $V_{n-1}^{+}$to V_1^{+} , as shown in **Equation 11.**

$$V_0 = V_i + V_{n-1}^{+} + V_{n-3}^{+} + V_{n-5}^{+} \cdots + V_1^{+} \quad (11)$$

By summarizing **Equation 3-11**, **Equation 12** describe the total value of the output voltage (V_0).

$$V_i = V_i$$

$$+V_{n-1}^{+} = V_{n-1}^{-} - \frac{\frac{n}{2}\Delta Q}{C_{n-1}}$$

$$+V_{n-3}^{+} = 2V_i - \frac{\frac{n}{2}\Delta Q}{C_{n-1}} - \frac{\left(\frac{n}{2}-1\right)\Delta Q}{C_{n-2}} - \frac{\left(\frac{n}{2}-1\right)\Delta Q}{C_{n-3}}$$

$$\vdots \qquad \vdots \qquad \vdots \qquad \vdots \qquad \vdots$$

$$+V_1^{+} = 2V_i - \frac{\frac{n}{2}\Delta Q}{C_{n-1}} - \frac{\left(\frac{n}{2}-1\right)\Delta Q}{C_{n-2}} - \frac{\left(\frac{n}{2}-1\right)\Delta Q}{C_{n-3}} - \frac{\left(\frac{n}{2}-2\right)\Delta Q}{C_{n-4}} - \frac{\left(\frac{n}{2}-2\right)\Delta Q}{C_{n-5}} - \cdots \frac{\Delta Q}{C_2} - \frac{\Delta Q}{C_1}$$

$$= V_0 = nV_i - \frac{\left(\frac{n}{2}\right)^2 \Delta Q}{C_{n-1}} - \frac{\left(\frac{n}{2}-1\right)^2 \Delta Q}{C_{n-2}} - \frac{\left(\frac{n}{2}-1\right)^2 \Delta Q}{C_{n-3}} - \frac{\left(\frac{n}{2}-2\right)^2 \Delta Q}{C_{n-4}} - \frac{\left(\frac{n}{2}-2\right)^2 \Delta Q}{C_{n-5}} - \cdots \frac{\Delta Q}{C_2} - \frac{\Delta Q}{C_1} \quad (12)$$

the multiplication of frequency *f* and charge ΔQ is equal to the output current of the CW circuit I_0. This relationship can give the final form of **Equation 12** into **Equation 13**.

$$V_0 = nV_i - \left[\frac{\left(\frac{n}{2}\right)^2}{C_{n-1}} - \frac{\left(\frac{n}{2}-1\right)^2}{C_{n-2}} - \frac{\left(\frac{n}{2}-1\right)^2}{C_{n-3}} - \frac{\left(\frac{n}{2}-2\right)^2}{C_{n-4}} - \frac{\left(\frac{n}{2}-2\right)^2}{C_{n-5}} - \cdots \frac{1}{C_2} - \frac{1}{C_1}\right]\frac{I_0}{f} \quad (13)$$

If *n* is equal to or larger than 4, equation 11 can be further simplified to **Equation 14** as follows:

$$V_{0(n>4)} \cong nV_i - \frac{n^3}{12Cf} I_0 \quad (14)$$

Equation 14 shows that the output voltages depend much on the number of capacitors in the CW voltage multiplier. **Equation 14** also shows that large *n* may increase the internal resistance. According to **Equation 14,** the source resistance may increase as the cube of the multiplication. There is also a possibility of the stray shunt capacitance effect in the more stages of the CW circuit. This stray shunt capacitance effect allows the AC voltage to flow directly to the capacitor, which can reduce the output voltage of the CW circuit [39]. CW voltage multiplier circuit does not multiply the power. In principle, the power supplied by the power source and the output power should be the same. This means that the output voltage can be very high, and the output current gets smaller. This CW multiplier circuit

type is suitable for devices requiring only high voltage and low currents. In this case, we select this CW circuit as a universal platform for DEAs testing and education. CW voltage has a much simpler configuration than dc/dc converter or an HV generator that uses a transformer. CW voltage only requires capacitors and diodes to multiply a relatively low voltage to a high voltage while maintaining a simpler configuration.

2.2. High voltage Amplifier based on a CW circuit

In this study, we designed a CW circuit based on the required output dc voltage. VHB (Very high bond tape from VHB Y-4905J; 3M, Maplewood, MN, USA) based DEAs require at least 2 kV for the actuation. In this case, the CW design should have an output of at least 2kV. In Japan, the normal AC power source is 110V. Connecting directly to the AC power source may need many stages to achieve 2kV. Additionally, the platform may only work in a certain region. The strategy is to use more general equipment, such as DC adaptor to achieve a universal platform for DEAs testing,

In this research, we used a 12V DC voltage adaptor. To convert the DC to AC, we used a low-cost DC-AC inverter (DC12V cold cathode tube inverter set from Akizuki Denshi Tsusho Co. , Ltd.). This device can amplify the DC 12V to approximately 524V peak-to-peak AC voltage at approximately 77.4 kHz. Figure 2a shows the UHV-Amp device arrangement. In Figure 2a, we used several additional components, such as Arduino micro, L298N (voltage regulator), and optocoupler, to control the amplified voltage output. In this UHV-Amp, Arduino works to control the L298N. We used a PWM signal to control the voltage regulator L298N, which also resulted in the controlled voltage input to the DC-AC inverter. We used module L298N because it has some features including support independent electric power source up to 12 VDC, maximum voltage output is also 12 VDC and can be easily regulated using PWM pin from Arduino. We also can set the output of the DC voltage into square wave DC voltage using two functions. First, we can set the Arduino to have a square wave and the final output voltage is a square wave and low frequency. Second, we can use the optocoupler as a switching device to generate square wave DC Voltage with a higher frequency.

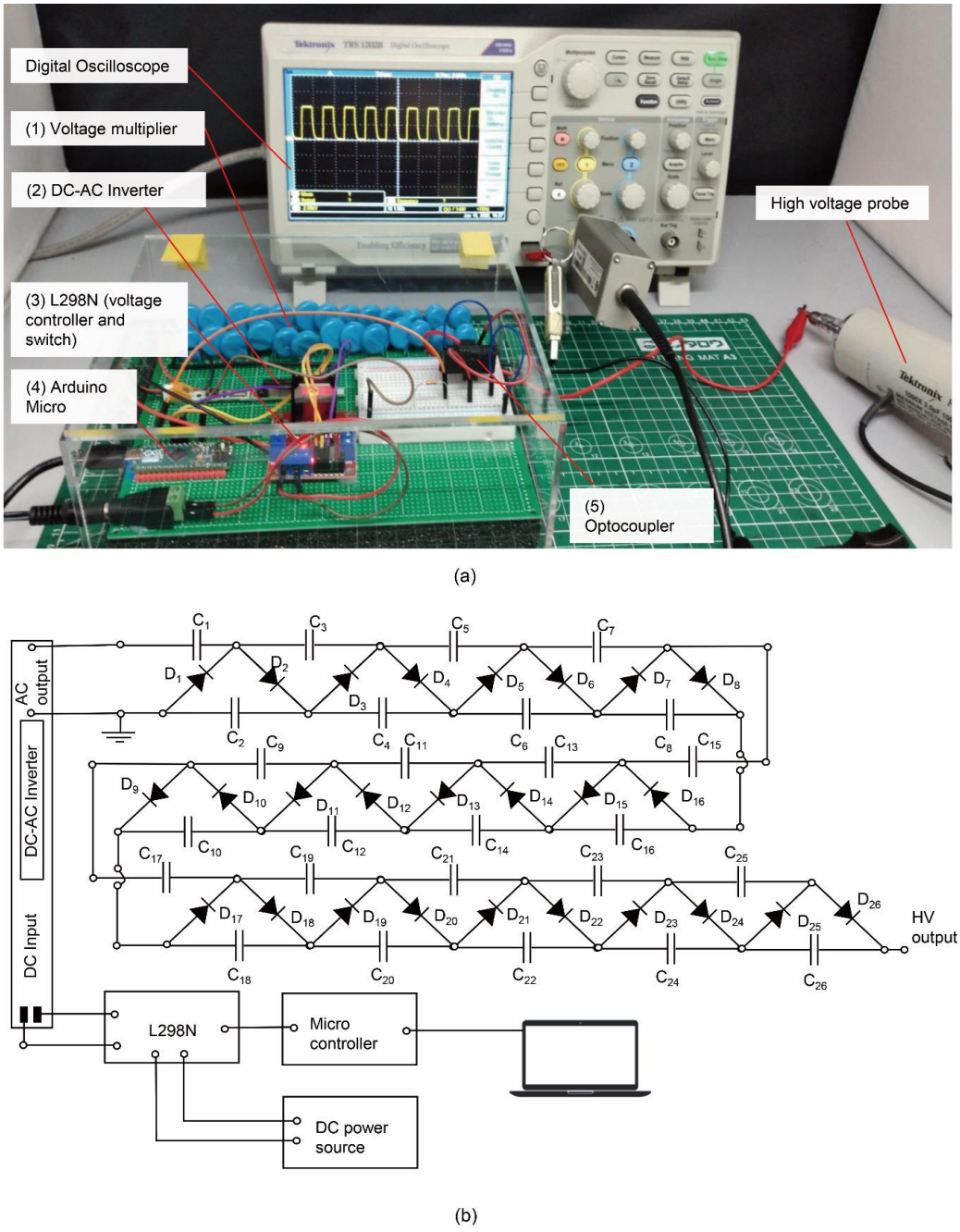

Figure 3. Universal Platform of Ladder-Based Network Voltage Amplifier (a. Voltage amplifier, b. Electric circuit schematic of the voltage Amplifier)

Figure 3b shows the schematic of the UHV-Amp. The main CW circuit in UHV-Amp consists of 26 capacitors (each capacitor was 2200PF with a voltage rating of 10kV) and 26 diodes (with a voltage rating of 20kV). Theoretically, this schematic is equal to 13 steps of a CW circuit. The main power of the CW circuit comes from a 12V DC power source. The DC power passes through the voltage regulator L298N. We controlled the voltage regulator using a microcontroller. By controlling the voltage regulator, we can easily control the HV voltage output at the end of the system. The

regulated voltage from L298N flows through the DC-AC inverter. This DC-AC inverter can also amplify the DC voltage to 524V AC peak voltage. Then finally, the AC voltage passes through the CW circuit and is amplified to the kV range voltage output. By using these methods, our device can generate voltage of 4 kV at maximum. From **Equation 14,** the estimated output current was approximately 1.12 mA.

Figure 4 shows the logic control of the UHV-Amp. Every control schema has its own characteristics. For example: in **Figure 4a**, the frequency of the output DC voltage was controlled using L298N. Doing so makes the output voltage smooth but can only accommodate a low-frequency square wave DC-voltage output. On the other hand, in **Figure 4b,** the switching part is the optocoupler (DEAN OPC10M). The device can emit high-frequency DC voltage by using the optocoupler. However, the schema in Figure 3b may not be stable at the lower output frequency. In this research, we combine both devices to accommodate high-frequency DEAs testing and low-frequency DEAs testing. Next, to ease the user to operate UHV-Amp, we create a simple open-source graphic user interface (GUI) using Python. Open-source software should ensure the community can easily access this device and software. We expect our UHV-Amp can support the education of soft robotics.

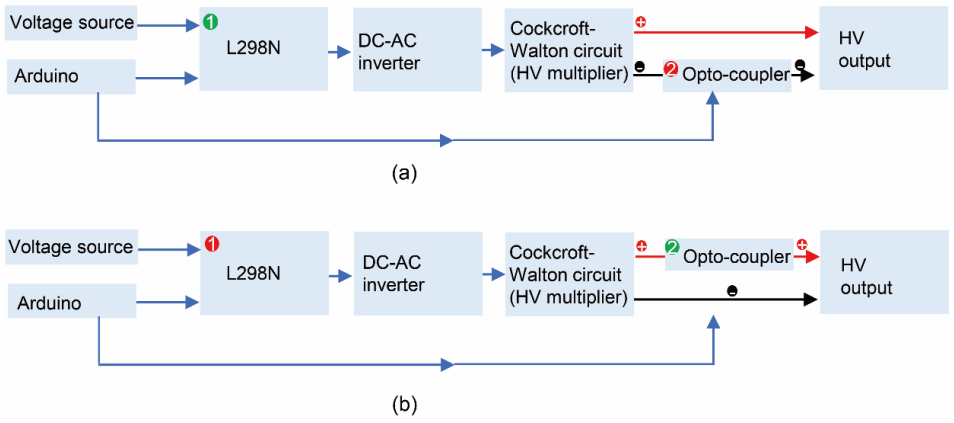

Figure 4. Control flow chart of the UHV-Amp (a. Controlling from L2986N (L298N is a voltage regulator and switch at the same time. As it is controlled using Arduino), b. Controlling from Optocoupler (the positive part was used as a switch))

3. Result

The previous chapter discussed two control methods of the UHV-Amp. We can control the voltage from the voltage regulator side (**Figure 4a**) for low-frequency operation and from the optocoupler (**Figure 4b**) for high-frequency operation. The UHV-Amp has two switching methods, as shown in **Figure 4**. When the DEAs testing requires a high-frequency or low-frequency operation, the block diagram with a green-colored-number becomes the switch, and the block diagram with a red-colored-number is in normally closed state. Our self-developed GUI can define the switch based on our frequency operation. **Figures 5a, b** and **c** show **0.25 Hz, 1Hz** and **5 Hz** output frequencies of the UHV-Amp, respectively. For low-frequency operations of 0.25 and 1 Hz, the wave can get to the initial position successfully. In the case of 5Hz, there is a gap g between zero Volt to the lower part of the graphic (**Figure 5c**). This gap g describes the offset voltage (V_g). This V_g appears due to the delay Δt at the charging and discharging positions (**Figure 5e**). Since in this schema, the controlling part is from the DC voltage source, there is a possibility of discharging and charging time delays from the capacitor.

This charge and discharge time delay limits the output frequency of the HV-output. **Figure 5d** shows the growth of V_g when the device is operated at a higher frequency. **Figure 5d** also indicates that the UHV-Amp has a low V_g in the operation range of 0-2Hz.

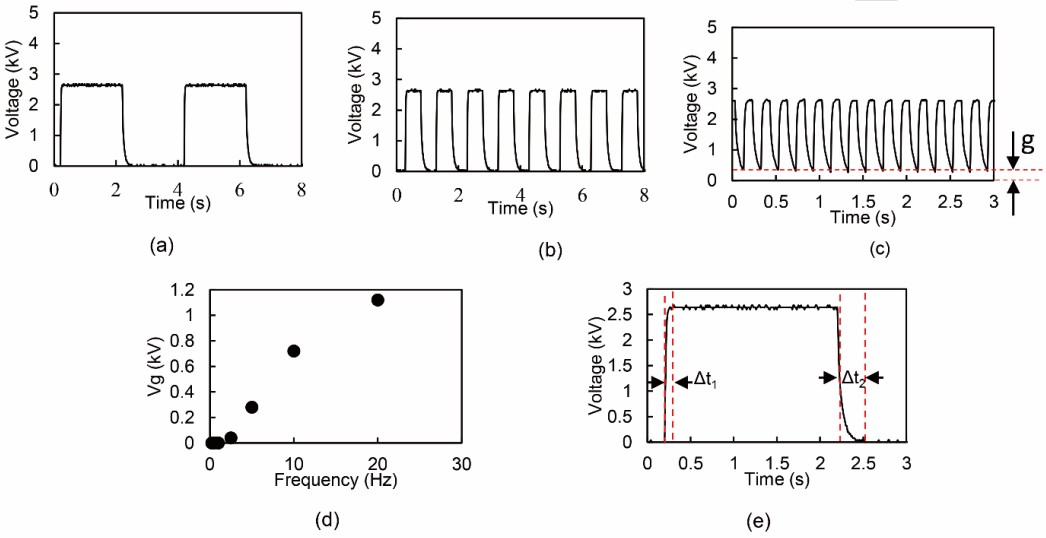

Figure 5. Low-frequency output voltage characteristics from the HV device (a. 0.25Hz, b. 1Hz, c. 5Hz, d. Gap (g) increase due to the increase of frequency, and e. relaxation time (Δt) of the HV device)

For higher frequency operation, we used schema 2 (**Figure 4b**) to control the output of the UHV-Amp. Since we controlled the UHV-Amp from the HV output part, the capacitor in the CW circuit does not need a charging and discharging process. By using this method, the device can achieve higher frequency operations. **Figures 6a** and **c** show the output voltage at 25Hz and 50 Hz, respectively. The gap g shown in **Figure 6b** is the offset voltage (V_g). V_g starts to appear at a frequency of 100Hz (Figure **6b**). **Figure 6d** shows the V_g growth due to the increase of the frequency. **Figure 6d** also indicates that the higher voltage (for example, 3kV) can also increase the V_g at a high-frequency operation.

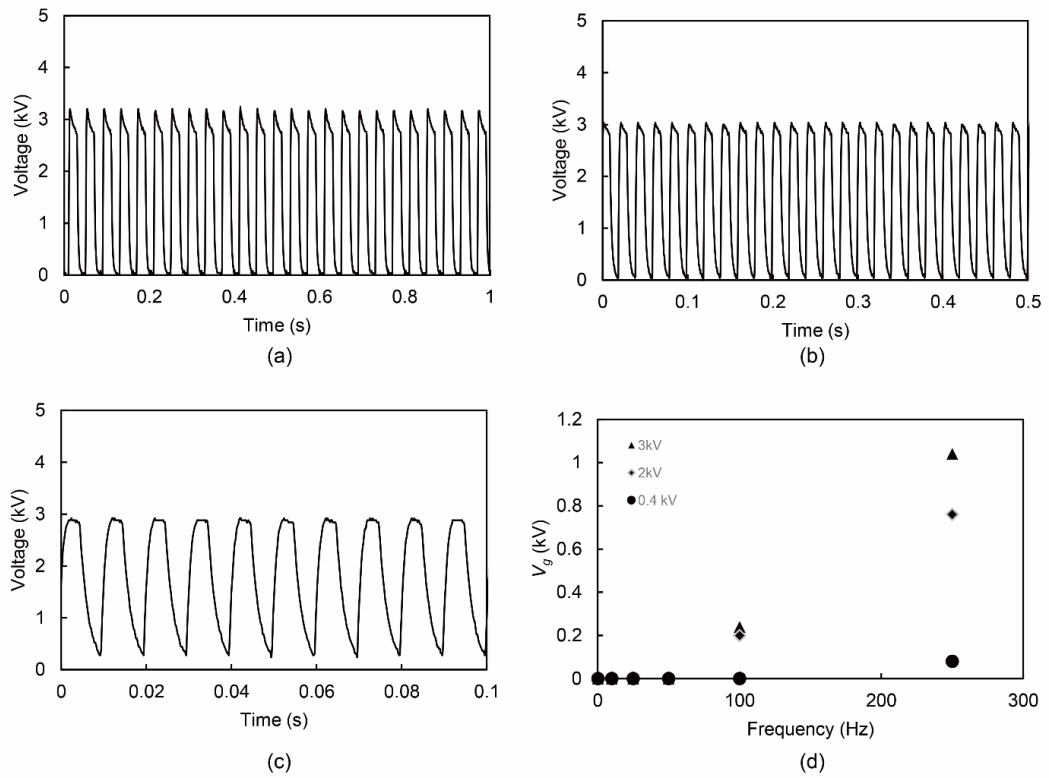

Figure 6. Higher frequency output voltage characteristics from HV device (a. 25Hz, b. 50Hz, c. 100Hz, and d. Gap (g) increase due to the increase of frequency)

In this research, we accommodate both low-frequency operation and high-frequency operation. In order to ease the user to control the UHV-Amp, we created a simple graphic user interface (GUI) using Python. This software is an open-source, and we put the source code in the supplementary information. **Figure 7** presents the GUI for the HV device. In this GUI, we accommodate static tests of DEAs, dynamic low frequency of DEAs, and dynamic high frequency of DEAs. Basically, the GUI interacts with the Arduino Micro. The Python GUI send certain code to activate the array function in the Arduino. In Arduino side, we put an array function consisting of high frequency and low frequency command of the UHV AMP. The basic programming algorithm for the high frequency and low frequency operation in the Arduino side is presented in Figure 4. Basically, without python GUI, we can control the UHV-AMP using ASCII command from Arduino IDE. The GUI is purposed to ease the user to operate the UHV AMP. For stability, we limit the voltage to a maximum of 3 kV.

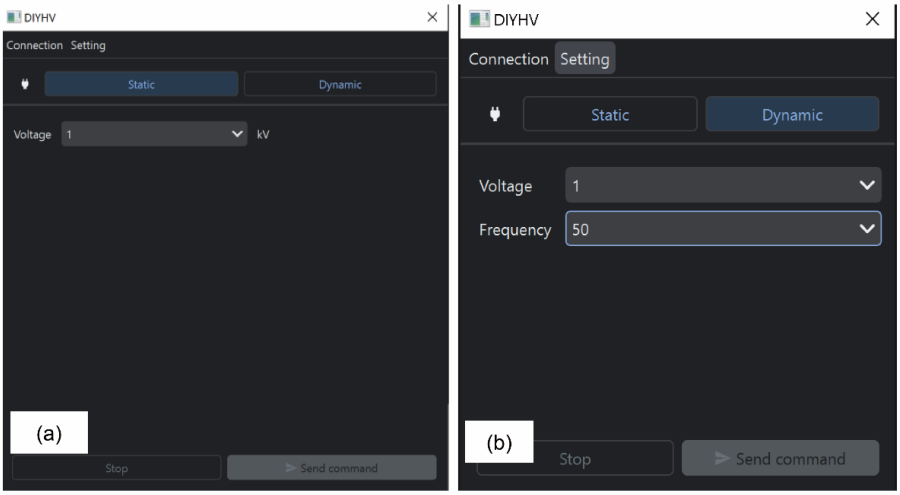

Figure 7. Simple GUI to control HV device

The GUI is straightforward. **Figure 7a** shows the static test windows, while **Figure 7b** shows the dynamic ones. First, we should connect the UHV-Amp to the personal computer (PC) by clicking the connection button. The communications between the PC and the UHV-Amp are through the serial port. Once the UHV-Amp is connected to the GUI, we can control the device easily. We can use the static tab to do a static DEAs test. By selecting the voltage value and pressing the send command button, the UHV-Amp can generate the selected voltage value. The same thing goes for the dynamic test. The device can generate the desired voltage and frequency by selecting the dynamic tab, putting the voltage and frequency values then pressing the send command button. For more detailed operation, **Movie S1** shows the GUI operation methods.

4. Discussion

The strong points of the CW circuit-based voltage amplifiers are the simplicity of the structure, lightweight, relatively low-cost, open source and high reproducibility. Our UHV-Amp consists of commercially available components. We can easily find the component in the marketplace and at a relatively low cost. For example, the capacitor was 2200pF with a voltage rating of 10 kV. This type of capacitor costs around $5.65 for a piece. Twenty-six capacitors cost $147. Then the diode (voltage rating of 20kV) costs around $11 for 26 pieces. Next, the DC-AC inverter costs around $1.12. Then the voltage regulator (L298N), Arduino micro, and the 12VDC power adaptor cost for $2.9, $24.47, $11.9, respectively. The optocoupler part is a choice, if the operator requires high frequency, adding the optocoupler may cost around $75. The total cost of our HV device was approximately $273.39.

This relatively low-cost device is suitable for the DIY project, especially for soft robotics education. The comparison of the UHV-Amp to other device is presented in **table 1**. Since all components can be easily found in a marketplace, this equipment also supports distance learning, where students can do a hands-on project. Further price reduction is possible by changing the microcontroller and optocoupler types. Currently, we use an optocoupler with a voltage rating of 10kV, while the UHV-Amp output is 3kV. By using a lower voltage rating of the optocoupler, we can further reduce the total price of the HV device.

Limitation in the UHV-AMP is the gap g that appear in high frequency operation as shown in **Figure 6b**. This gap is actually an offset voltage (Vg). In high frequency mode of UHV-AMP, Vg starts to appear at a frequency of 100Hz (**Figure 6c**). The Vg growth due to the increase of the frequency (**Figure 6d**). In this case, operation of UHV-AMP at higher frequency than 100Hz can induce Vg. Vg

cause a gap as shown in figure 6c. In some cases that require a perfect cyclic test condition in high frequency, we need to improve the electronics system, capacitor type and the grounding system in the UHV-AMP. By doing so, we expect the UHV-AMP to operate at higher frequency without any Vg.

For a comparison of our self-developed HV device to the professional version of the HV amplifier (Matsuda AMPS-20B20 from Matsuda Precision Inc), we connected VHB-type DEAs to both HV devices. The Matsuda AMPS-20B20 is the provisional device that we previously used to test dynamics and static performance of silicone type DEAs [13]. Matsuda AMP-20B20 has capability to produce up to 20kV DC, fast response of 4kHz full scale and 10% of full-scale up to 20kHz. **Figure 8** shows the actuation of DEAs when the DEAs are connected to the different high-voltage amplifiers. Both **Figure 8a** and **b** indicate that the actuation of the DEA does not have any significant difference. **Movie S2** shows the actuation of DEA using both of the equipment.

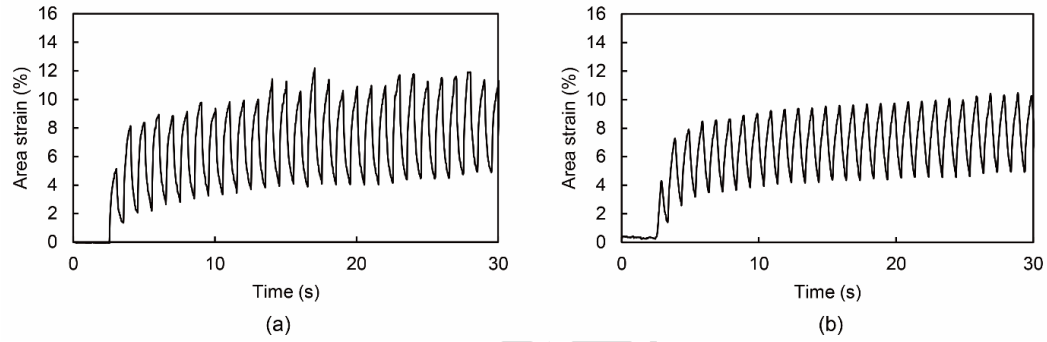

Figure 8. Dynamic actuation of VHB type DEAs at 2kV using a. Professional HV amplifier, b. Our HV experimental device.

Table 1. Voltage amplifier and DC-DC converter that is available in the marketplace

Type	Sample	Price (USD)	Source
High voltage amplifier	AMPS-20B20	+/- 46000	[40]
DC-DC Converter	Q30-12	+/-263	[41]
	A30P-5	+/-230	[42]
	UMHV0550	+/-312	[43]
	URT-5P-24	+/-480	[44]
Other	Peta-pico-Voltron: An open-source high-voltage power supply	420	[45]
High voltage amplifier	UHV-Amp	273.39	This research

5. Conclusion

In summary, the development of a universal platform of a ladder-based network voltage amplifier for DEAs testing is a significant step toward soft robotics education and technology. Since the UHV-Amp is relatively low-cost, light in weight, simple in structure, and high portability, newcomer researchers can easily access the UHV-Amp. All parts of the UHV-Amp are also available in the marketplace. This situation can support the student hands on project where distant learning is required. In this research, we used a 12V DC power source to power up the UHV-Amp and the maximum output voltage was 4kV. We limited the device to a 3kV output voltage to achieve the

stability output at high-frequency operation. From the viewpoint of safety, UHV-Amp is relatively safe because we used only 12 V DC as the power source and the CW circuit does not multiply the power. In this case, the voltage output becomes ultrahigh and the current is extremely low. According to the previous report, DC high voltage is also relatively safer than AC voltage. From the DEA actuation test, we found that our HV device is capable and comparable to the professional version of the HV amplifier. Additionally, we provide the GUI to control the device and the source code for the Arduino programming. We expect that our HV device can contribute to the education of soft robotics and speed up the development of soft robotics technologies. Our device also can support a general testing platform for different soft actuators such as shape memory polymer, shape memory alloy, electro adhesion and electrohydrodynamic pump (EHD). In the future we aim to improve the stability of our device at higher frequencies. In higher frequencies (e.g 1kHz), a DEAs can turn in to a speaker. Operating a DEAs at high frequencies is one future challenge for our UHV-AMP development.

Acknowledgments

This work was supported by Japan Society for the Promotion of Science for their support under Grants-in-Aid for Scientific Research on Innovative Areas (18H05473), and by JSPS KAKENHI (21J15489 and 23K13290).

Reference:

[1] Duduta M, Wood RJ, Clarke DR. Multilayer Dielectric Elastomers for Fast, Programmable Actuation without Prestretch. Adv Mater 2016;28:8058–63. https://doi.org/10.1002/adma.201601842.

[2] Kobayashi R, Nabae H, Suzumori K. Large Torsion Thin Artificial Muscles Tensegrity Structure for Twist Manipulation. IEEE Robot Autom Lett 2023;8:1207–14. https://doi.org/10.1109/LRA.2023.3236889.

[3] Fang Y, Zhang J, Xu B, Mao Z, Li C, Huang C, et al. Raising the Speed Limit of Axial Piston Pumps by Optimizing the Suction Duct. Chinese J Mech Eng 2021;34:105. https://doi.org/10.1186/s10033-021-00624-w.

[4] Cacucciolo V, Shintake J, Kuwajima Y, Maeda S, Floreano D, Shea H. Stretchable Pumps for Soft Machines. Nature 2019;572:516–9. https://doi.org/10.1038/s41586-019-1479-6.

[5] Mao Z, Iizuka T, Maeda S. Bidirectional electrohydrodynamic pump with high symmetrical performance and its application to a tube actuator. Sensors Actuators A Phys 2021;332:113168. https://doi.org/10.1016/j.sna.2021.113168.

[6] Shintake J, Rosset S, Schubert B, Floreano D, Shea H. Versatile Soft Grippers with Intrinsic Electroadhesion Based on Multifunctional Polymer Actuators. Adv Mater 2016;28:231–8. https://doi.org/10.1002/adma.201504264.

[7] Miao W, Zou W, Jin B, Ni C, Zheng N, Zhao Q, et al. On demand shape memory polymer via light regulated topological defects in a dynamic covalent network. Nat Commun 2020;11:1–8. https://doi.org/10.1038/s41467-020-18116-1.

[8] Mao Z, Shimamoto G, Maeda S. Conical frustum gel driven by the Marangoni effect for a motor without a stator. Colloids Surfaces A Physicochem Eng Asp 2020:125561. https://doi.org/10.1016/j.colsurfa.2020.124658.

[9] Mao Z, Kuroki M, Otsuka Y, Maeda S. Contraction waves in self-oscillating polymer gels. Extrem Mech Lett 2020;39:100830. https://doi.org/10.1016/j.eml.2020.100830.

[10] Shigemune H, Maeda S, Cacucciolo V, Iwata Y, Iwase E, Hashimoto S, et al. Printed Paper

Robot Driven by Electrostatic Actuator. IEEE Robot Autom Lett 2017;2:1001–7. https://doi.org/10.1109/LRA.2017.2658942.

[11] Hosoya N, Masuda H, Maeda S. Balloon dielectric elastomer actuator speaker Balloon dielectric elastomer actuator speaker. Appl Acoust 2019;148:238–45. https://doi.org/10.1016/j.apacoust.2018.12.032.

[12] Wiranata A, Kanno M, Chiya N, Okabe H, Horii T, Fujie T, et al. High-frequency oscillations of low-voltage dielectric elastomer actuators. Appl Phys Express 2021;15:011002–1.

[13] Wiranata A, Ishii Y, Hosoya N, Maeda S. Simple and Reliable Fabrication Method for Polydimethylsiloxane Dielectric Elastomer Actuators Using Carbon Nanotube Powder Electrodes. Adv Eng Mater 2021;23:1–11. https://doi.org/10.1002/adem.202001181.

[14] Belforte G, Eula G, Ivanov A, Sirolli S. Soft pneumatic actuators for rehabilitation. Actuators 2014;3:84–106. https://doi.org/10.3390/act3020084.

[15] Blanes C, Mellado M, Beltran P. Novel additive manufacturing pneumatic actuators and mechanisms for food handling grippers. Actuators 2014;3:205–25. https://doi.org/10.3390/act3030205.

[16] Marín D, Llano-viles J, Haddi Z, Perera-lluna A, Fonollosa J, Mar D. system Jou rna lP. Sensors Actuators B Chem 2023:134036. https://doi.org/10.1016/j.birob.2023.100127.

[17] Shigemune H, Sugano S, Nishitani J, Yamauchi M, Hosoya N, Hashimoto S, et al. Dielectric Elastomer Actuators with Carbon Nanotube Electrodes Painted with a Soft Brush. Actuators 2018;7:1–11. https://doi.org/10.3390/act7030051.

[18] Hosoya N, Baba S, Maeda S. Hemispherical breathing mode speaker using a dielectric elastomer actuator. J Acoust Soc Am 2015;138:EL424–8. https://doi.org/10.1121/1.4934550.

[19] Tan MWM, Thangavel G, Lee PS. Enhancing Dynamic Actuation Performance of Dielectric Elastomer Actuators by Tuning Viscoelastic Effects with Polar Crosslinking. NPG Asia Mater 2019;11:62. https://doi.org/10.1038/s41427-019-0147-5.

[20] Murakami T, Kuwajima Y, Wiranata A, Minaminosono A, Shigemune H, Mao Z, et al. A DIY Fabrication Approach for Ultra - Thin Focus - Tunable Liquid Lens Using Electrohydrodynamic Pump. Micromachines 2021;12:1–10.

[21] Mao Z, Asai Y, Yamanoi A, Seki Y, Wiranata A, Minaminosono A. Fluidic rolling robot using voltage-driven oscillating liquid. Smart Mater Struct 2022;31. https://doi.org/10.1088/1361-665X/ac895a.

[22] Mao Z, Peng Y, Hu C, Ding R, Yamada Y, Maeda S. Soft computing-based predictive modeling of flexible electrohydrodynamic pumps. Biomim Intell Robot 2023;3:100114. https://doi.org/https://doi.org/10.1016/j.birob.2023.100114.

[23] Matsuo H, Harada K. The Cascade Connection of Switching Regulators. IEEE Trans Ind Appl 1976;IA:192–8.

[24] Seeman MD. A Design Methodology for Switched-Capacitor DC-DC Converters 2009.

[25] Ali EM, Yahaya NZ, Saraereh OA, Assaf AH Al, Alqasem BH, Iqbal S, et al. Power conversion using analytical model of cockcroft- walton voltage multiplier rectenna. Electron 2021;10:1–16. https://doi.org/10.3390/electronics10080881.

[26] Siwakoti YP, Member S, Peng FZ, Blaabjerg F, Loh PC, Town GE, et al. Impedance-Source Networks for Electric Power Conversion Part I : A Topological Review. IEEE Trans Power Electron 2015;30:699–716. https://doi.org/10.1109/TPEL.2014.2313746.

[27] Forouzesh M, Siwakoti YP, Gorji SA, Blaabjerg F, Lehman B. A survey on voltage boosting

techniques for step-up DC-DC converters. ECCE 2016 - IEEE Energy Convers Congr Expo Proc 2016. https://doi.org/10.1109/ECCE.2016.7854792.

[28] Wiranata A, Ohsugi Y, Minaminosono A, Mao Z, Kurata H, Hosoya N, et al. A DIY Fabrication Approach of Stretchable Sensors Using Carbon Nano Tube Powder for Wearable Device. Front Robot AI 2021;8:1–15. https://doi.org/10.3389/frobt.2021.773056.

[29] Vallejo W, Diaz-Uribe C, Fajardo C. Do-it-yourself methodology for calorimeter construction based in Arduino data acquisition device for introductory chemical laboratories. Heliyon 2020;6:e03591. https://doi.org/10.1016/j.heliyon.2020.e03591.

[30] Grinias JP, Whitfield JT, Guetschow ED, Kennedy RT. An inexpensive, open-source USB Arduino data acquisition device for chemical instrumentation. J Chem Educ 2016;93:1316–9. https://doi.org/10.1021/acs.jchemed.6b00262.

[31] Shin JH, Choi S. Open-source and do-it-yourself microfluidics. Sensors Actuators B Chem 2021;347:130624. https://doi.org/10.1016/j.snb.2021.130624.

[32] Kubínová Š, Šlégr J. ChemDuino: Adapting Arduino for Low-Cost Chemical Measurements in Lecture and Laboratory. J Chem Educ 2015;92:1751–3. https://doi.org/10.1021/ed5008102.

[33] Tvarijonaviciute A, Carrillo-Sanchez JD, Rubio CP, Contreras-Aguilar MD, Muñoz-Prieto A, Pardo-Marin L, et al. Low-cost do-it-yourself (DIY) mannequin for blood collection: A comprehensive evaluation about its use in teaching. Res Vet Sci 2022;148:15–20. https://doi.org/10.1016/j.rvsc.2022.04.009.

[34] Tischler J, Swank Z, Hsiung HA, Vianello S, Lutolf MP, Maerkl SJ. An automated do-it-yourself system for dynamic stem cell and organoid culture in standard multi-well plates. Cell Reports Methods 2022;2:100244. https://doi.org/10.1016/j.crmeth.2022.100244.

[35] Aranganadin K, Zhang Z, Lin Y, Chang P, Hsu H, Lin M, et al. A Mini-Marx Generator Powered by a Cockcroft – Walton Voltage Multiplier. IEEE Trans Plasma Sci 2022;50:3393–9.

[36] Everhart E, Lorrain P. The Cockcroft-Walton voltage multiplying circuit. Rev Sci Instrum 1953;24:221–6. https://doi.org/10.1063/1.1770669.

[37] Holland DP, Park EJ, Polygerinos P, Bennett GJ, Walsh CJ. The Soft Robotics Toolkit: Shared Resources for Research and Design. Soft Robot 2014;1:224–30. https://doi.org/10.1089/soro.2014.0010.

[38] Brugler J. Theoretical Performance of Voltage Multiplier Circuits. IEEE J Solid-State Circuits 1971;6:132–5. https://doi.org/10.1109/JSSC.1971.1049670.

[39] Cockcroft JD, Walton ETS. Experiments with High Velocity Positive Ions Email alerting service. Proceeding R. Soc. A, vol. 129, 1930. https://doi.org/https://doi.org/10.1098/rspa.1932.0107.

[40] AMP-20B20 2023. https://www.matsusada.com/product/amp/hiv/amp/ (accessed February 5, 2023).

[41] Q30-12 n.d. https://www.digikey.my/en/products/detail/xp-power/Q30-12/5873636 (accessed February 6, 2023).

[42] A30P-5 n.d. https://www.digikey.my/en/products/detail/xp-power/A30P-5/5873510 (accessed February 2, 2023).

[43] UMHV0550 n.d. https://www.digikey.jp/ja/products/detail/hvm-technology-inc/UMHV0550/10707950 (accessed February 6, 2022).

[44] URT-5P-5 n.d. https://www.matsusada.com/product/hvps2/onboard/urt/ (accessed February 6,

2023).

[45] Schlatter S, Illenberger P, Rosset S. Peta-pico-Voltron: An open-source high voltage power supply. HardwareX 2018;4:e00039. https://doi.org/10.1016/j.ohx.2018.e00039.